

Partial Identification with Noisy Covariates: A Robust Optimization Approach

Wenshuo Guo[†], Mingzhang Yin[◇], Yixin Wang^{*}, Michael I. Jordan^{†,‡}

[†]Department of Electrical Engineering and Computer Sciences, University of California, Berkeley

[◇] Data Science Institute, Columbia University

^{*} Department of Statistics, University of Michigan

[‡]Department of Statistics, University of California, Berkeley

February 23, 2022

Abstract

Causal inference from observational datasets often relies on measuring and adjusting for covariates. In practice, measurements of the covariates can often be noisy and/or biased, or only measurements of their proxies may be available. Directly adjusting for these imperfect measurements of the covariates can lead to biased causal estimates. Moreover, without additional assumptions, the causal effects are not point-identifiable due to the noise in these measurements. To this end, we study the partial identification of causal effects given noisy covariates, under a user-specified assumption on the noise level. The key observation is that we can formulate the identification of the average treatment effects (ATE) as a robust optimization problem. This formulation leads to an efficient robust optimization algorithm that bounds the ATE with noisy covariates. We show that this robust optimization approach can extend a wide range of causal adjustment methods to perform partial identification, including backdoor adjustment, inverse propensity score weighting, double machine learning, and front door adjustment. Across synthetic and real datasets, we find that this approach provides ATE bounds with a higher coverage probability than existing methods.

1 Introduction

Estimating the causal effect of an intervention is a problem that arises in countless domains, with examples including identifying the effect of medical treatments (Connors et al., 1996), evaluating the effectiveness of recommender systems (Schnabel et al., 2016; Wang et al., 2020), and assessing the impact of educational methods (Gustafsson, 2013). In many of these settings, the challenge is to identify causal effects from observational data, and a core problem is that naive inference can be biased by *confounders*, which are variables that affect both the intervention and the outcomes. For example, in identifying the effect of college education on earnings for students, the scholastic ability is a confounder (Card, 1999)—it can affect both whether the student can be admitted to a college and how much he/she may earn after graduation. As a result, the observed increase in earnings associated with attending college is confounded by the effect of the scholastic ability and thus cannot accurately represent the causal effect of college education.

A common approach to addressing confounding bias is aiming to measure all of the confounders and adjust for them (Imbens and Rubin, 2015). In practice, however, measurements of the confounders can often be noisy or biased. Moreover, sometimes we only have access to proxies of the confounders. For instance, in the example of college education and earnings, confounders are often measured via surveys

and thus are typically biased and incomplete—participants may not be willing to discuss aspects of their family backgrounds or reveal their access to alternative educational or career options. Some confounders are difficult to measure by definition—for example, students’ innate cognitive abilities—and in such cases we generally only have access to proxies.

While noisy covariates (including both noisy measurements and confounder proxies) are generally needed to perform causal inference, directly adjusting for such covariates can lead to biased causal estimates (Fuller, 2009). Moreover, it is well known that, without further assumptions on the causal model, the causal effects are not point-identifiable given only noisy covariates (Carroll et al., 2006; Schennach, 2016; Ogburn and Vanderweele, 2013; Lockwood and McCaffrey, 2016). In other words, with access to only noisy covariates, it may be impossible to pinpoint the causal effect of interest even with infinite data. How then can noisy covariates inform causal inference?

In this paper, we leverage the noisy covariates to perform partial identification of the causal effects. Given a user-specified assumption on the noise level, we develop an algorithm for partial identification using robust optimization. This approach capitalizes on two observations: (1) the causal effects of interest are identifiable given the (unobserved) true joint distribution of treatments, outcomes, and all (noiseless) covariates; (2) the dataset with noisy covariates places constraints on what this joint distribution can be. These observations allow us to turn the task of partial identification into a robust optimization problem.

In more detail, we formulate partial identification as the following robust optimization problem. We first consider an uncertainty set of all possible underlying joint distribution of treatments, outcomes, and the noiseless covariates subject to the constraints. Then we find the maximum (or minimum) possible causal effects that a distribution in this set can plausibly lead to. This approach propagates the uncertainty in the true data distribution (due to covariate noise) downstream to the uncertainty in the causal estimation, leading to partial identification intervals of the causal effects.

Taking this optimization perspective on partial identification, we develop an algorithm that efficiently solves the robust optimization problem and computes the bounds on the causal effect of interest. This algorithm is applicable to a wide variety of causal adjustment methods, including backdoor adjustment, frontdoor adjustment, inverse propensity score weighting (IPW), and double machine learning, which we demonstrate. Across simulated and real datasets, we find that this approach can produce tight bounds on causal effects that cover the true average treatment effect.

Contributions. We propose a robust optimization approach to partial identification given noisy covariates. The key idea is to formulate partial identification with noisy covariates as a robust optimization problem. We provide an efficient algorithm to solve this robust optimization program, thereby obtaining upper and lower bounds on the causal effects. We demonstrate the general applicability of this approach by applying it to a variety of causal adjustment methods. Finally, we demonstrate the effectiveness of the approach across empirical studies with synthetic and real data.

Related work. This work draws on several threads of research in measurement noise, proxy variables, and robust optimization.

The first is on measurement noise and proxy variables in causal inference. This subject has a long history in the literature (Wickens, 1972; Frost, 1979), where there have been a variety of proposals for recovering causal effects either heuristically or with additional model assumptions (Carroll et al., 2006; Schennach, 2016; Ogburn and Vanderweele, 2013; Lockwood and McCaffrey, 2016). Recent examples include Louizos et al. (2017), who use variational autoencoders as a heuristic way to recover the latent confounders; and Kallus et al. (2018), who use matrix factorization to infer the confounders from the noisy covariates assuming that the data-generating process follows a linear outcome model. Given proxy vari-

ables of unmeasured confounders, [Kuroki and Pearl \(2014\)](#) and [Miao et al. \(2018\)](#) propose specific technical conditions under which causal effects can be restored. These results have been extended to a variety of other settings ([Tchetgen et al., 2020](#); [Shi et al., 2020](#); [Cui et al., 2020](#); [Shpitser et al., 2021](#); [Dukes et al., 2021](#); [Ying et al., 2021](#); [Shi et al., 2021](#)). Finally, [Imai and Yamamoto \(2010\)](#) seek to partially identify ATE under measurement error using constrained linear optimization. More recently, [Finkelstein et al. \(2020\)](#); [Duarte et al. \(2021\)](#); [Zhang et al. \(2021\)](#); [Zhang and Bareinboim \(2021b\)](#); [Balke and Pearl \(1994, 1997\)](#); [Ramsahai and Spirtes \(2012\)](#); [Bonet \(2013\)](#); [Heckman and Vytlačil \(2001\)](#); [Sachs et al. \(2020\)](#); [Geiger and Meek \(1999\)](#) develop optimization formulations for partial identification. Most of this work focuses on discrete variables under settings including unobserved confounding and/or measurement error. Our work is complementary to this work; we focus on noisy covariates but can handle certain settings with continuous variables, without relying on additional compliance assumptions.

Noisy covariates or proxy variables are not generally sufficient to identify causal effects as they violate the “no unobserved confounders” assumption. Therefore, handling noisy covariates relates to sensitivity analyses that seek partial identification; i.e., bounds on the average treatment effect (ATE) ([Liu et al., 2013](#); [Richardson et al., 2014](#); [Imbens, 2003](#); [Veitch and Zaveri, 2020](#); [Dorie et al., 2016](#); [Cinelli and Hazlett, 2020](#); [Cinelli et al., 2019](#); [Franks et al., 2019](#); [Shen et al., 2011](#); [Hsu and Small, 2013](#); [Bonvini and Kennedy, 2020](#); [Rosenbaum et al., 2010](#); [Zhao et al., 2017](#); [Yadlowsky et al., 2018](#); [Zhang and Bareinboim, 2021a](#); [Yin et al., 2021](#)). In this vein, the work of [Yadlowsky et al. \(2018\)](#) is most related. They propose a loss-minimization approach that quantifies bounds on the conditional average treatment effect (CATE). Their approach requires the unobserved confounder to satisfy a constraint that bounds the effect on the odds of treatment selection.

The second thread of related work concerns robust optimization, which is a core ingredient of the robust causal inference approach we develop. We adopt a minimax formulation of a two-player game where the uncertainty is adversarial, and one minimizes a worst-case objective over a feasible set ([Ben-Tal et al., 2009](#); [Bertsimas et al., 2011](#)). For example, the noise may be contained in a unit-norm ball around the input data. To solve the robust optimization problem, we build on a recent line of work on distributionally robust optimization (DRO) which assumes that the uncertain distributions underlying the data have support within a certain set ([Namkoong and Duchi, 2016](#); [Duchi and Namkoong, 2018](#); [Li et al., 2019](#)).

2 Preliminaries: Potential Outcomes, ATE Estimation, and Noisy Covariates

In this section, we set up the causal inference problem with noisy covariates and formalize the assumptions required by the partial identification of ATE.

Potential outcome and ATE estimation. Let $D^* = (X, Y, Z)$ denote a dataset, where X represents a vector of (possibly unobserved) noiseless covariates. Denote Z as a binary treatment random variable, with 0 and 1 being the labels for control and active treatments, respectively. Further, let Y denote the outcome. We use the potential outcomes notation to define causal quantities ([Neyman, 1923](#); [Rubin, 1974](#)): For each realization of the level of treatment, $z \in \{0, 1\}$, we assume that there exists a potential outcome, $Y(z)$, representing the outcome had the subject been given treatment z (possibly contrary to fact). Then, the observed outcome is $Y = Y(Z) = ZY(1) + (1 - Z)Y(0)$. We focus on estimating the average treatment effect (ATE):

$$\tau = \mathbb{E}[Y(1) - Y(0)]. \tag{1}$$

To focus on the causal inference challenge due to noisy covariates, we assume that the ATE is identifiable with the (potentially unobserved) noiseless data.

Assumption 1 (Identifiability of ATE given noiseless covariates) *The ATE is identifiable (Pearl, 1995) given the (unobserved) noiseless covariates, in addition to the observed treatment and outcome, namely the ATE can be written as a functional of the joint distribution of $D^* = (X, Y, Z)$.*

Assumption 1 ensures the identifiability of ATE if we had access to the noiseless covariates. This assumption is satisfied when the noiseless covariates X meet identification conditions for ATE such as the backdoor criterion, the positivity condition and weak unconfoundedness (Rosenbaum and Rubin, 1983), and the frontdoor criterion (Pearl, 2009).

Noisy covariates. Though the noiseless data $D^* = (X, Y, Z)$ can identify the ATE, we often do not have access to such a dataset. Instead, we only have access to a dataset with noisy covariates \tilde{X} . We denote the observed dataset as $D = (\tilde{X}, Y, Z)$.

The noisy covariates \tilde{X} shall potentially still provide information about X despite the noise. To describe to what extent can \tilde{X} inform X , we rely on an assumption about the noise level.

Assumption 2 (Noise level) *The TV distance between the distributions of X and \tilde{X} , conditional on the treatment variable Z , is bounded by a constant γ_z :*

$$\text{TV}(p_{x|z}, p_{\tilde{x}|z}) \leq \gamma_z, z \in \{0, 1\}, \quad (2)$$

where $p_{x|z}$ is the distribution of the unobserved noiseless covariates for the treatment or control group, $X|Z = z \sim p_{x|z}$, $p_{\tilde{x}|z}$ is the distribution of the noisy covariates \tilde{X} , $\tilde{X}|Z = z \sim p_{\tilde{x}|z}$, and the TV distance between two probability distributions p and q is defined as follows:

$$\begin{aligned} \text{TV}(p, q) &= \inf_{\pi} \mathbb{E}_{X, Y \sim \pi(x, y)} [\mathbb{1}(x \neq y)] \\ \text{s.t. } &\int \pi(x, y) dy = p(x), \int \pi(x, y) dx = q(y), \end{aligned} \quad (3)$$

where π represents a coupling between p and q (cf. Villani, 2008).

Assumption 2 provides a convenient way to characterize how far away the noisy covariates \tilde{X} are from their (unobserved) noiseless counterpart X , where the further away the noisy covariates \tilde{X} is from X , the less informative \tilde{X} is for causal inference. The upper bound of the TV distance γ_z in Assumption 2 is a user-specified parameter, which is often specified by domain experts or estimated from auxiliary datasets. In particular, the TV distance as a distance to quantify the noise level in Assumption 2 because of the computational tractability of TV distance in robust optimization, which we will detail in § 3 and appendix A.

Many existing noise models imply the TV bound on distributions in Assumption 2. We illustrate a few of these models below.

1. *Huber contamination model.* Suppose the noisy covariates deviate from the noiseless covariates following the Huber contamination model

$$p_{\tilde{x}|z} = (1 - \gamma_z)p_{x|z} + \gamma_z h_{\tilde{x}|z},$$

where $h_{\tilde{x}|z}$ can be any arbitrary distribution. Then the noisy covariates satisfy $\text{TV}(p_{x|z}, p_{\tilde{x}|z}) \leq \gamma_z$.

2. *Misclassification error.* Suppose the noisy covariates \tilde{X} are discrete and their misclassification error satisfies

$$\max_x \left| P(X = x|Z = z) - P(\tilde{X} = x|Z = z) \right| < \gamma_z, \quad z \in \{0, 1\}.$$

Then we also have $\text{TV}(p_{x|z}, p_{\tilde{x}|z}) \leq \gamma_z$.

3. *Exponential tilting model.* Suppose the distribution of \tilde{X} is an exponential tilted version of X , and both distributions belong to the exponential family,

$$p(x|z) = \exp(\eta(\theta_z) \cdot T(x) + A(\theta_z) + B(x)), \quad p(\tilde{x}|z) = \exp(\eta(\tilde{\theta}_z) \cdot T(\tilde{x}) + A(\tilde{\theta}_z) + B(\tilde{x})).$$

Then $\text{TV}(p_{x|z}, p_{\tilde{x}|z}) \leq \gamma_z \triangleq \sqrt{\frac{1}{2}D_A(\tilde{\theta}_z, \theta_z)}$, where $D_A(\cdot)$ is the Bregman divergence with function A (Banerjee et al., 2005).

4. *Other models.* For general noise models for \tilde{X} , one can approximately estimate the TV bound γ_z in [Assumption 2](#) by drawing samples from $p_{\tilde{x}|z}$ and $p_{x|z}$ respectively, calculating the KL divergence estimates (Pérez-Cruz, 2008; Belghazi et al., 2018), and applying Pinsker’s inequality.

Finally, [Assumption 2](#) specifies a noise-level assumption on the conditional distributions $p_{x|z}$ and $p_{\tilde{x}|z}$. One can similarly specify the noise level for the marginal distributions of the covariates, $p_x, p_{\tilde{x}}$, or the conditional distributions given both the treatments and the outcomes, $p_{x|y,z}, p_{\tilde{x}|y,z}$. Here we consider the use of $p_{x|z}$ and $p_{\tilde{x}|z}$ as a demonstrative example, formulating the partial identification task into a robust optimization problem in § 3. Similar derivations apply to versions of [Assumption 2](#) with other distributions.

3 Partial Identification with Noisy Covariates

Though [Assumption 1](#) ensures that the ATE is identifiable given the noiseless covariates X , the ATE is not point-identifiable without further assumptions given only the noisy covariates \tilde{X} —there exist many values of ATE that are all compatible with the observed distribution of D (Carroll et al., 2006; Schennach, 2016; Ogburn and Vanderweele, 2013; Lockwood and McCaffrey, 2016).

Given this lack of point identifiability, we focus on partial identification of ATE. Instead of providing a point estimate of the ATE, we aim to bound the ATE given the dataset with noisy covariates $D = (\tilde{X}, Y, Z)$. In particular, we develop an optimization approach to partial identification. The key idea is to cast the task of partial identification as a robust optimization problem. We consider the set of all joint distributions of the (unobserved) noiseless data $P(X, Y, Z)$ that are compatible with the observed noisy data $P(\tilde{X}, Y, Z)$ under the noise-level assumption ([Assumption 2](#)). Then the minimum and maximum value of ATE resulting from these joint distributions shall bound the ATE. It turns out that finding the minimum and maximum can be turned into a robust optimization problem, for which we develop an algorithm to solve.

In the rest of this section, we begin with the parametric approach to estimate ATE given noiseless data $D^* = (X, Y, Z)$; it can be written as an optimization problem as the parameter model is fitted via maximum likelihood. We then expand this optimization problem to consider the dataset with noisy covariates $D = (\tilde{X}, Y, Z)$, which results in a robust optimization problem. We will derive an efficient algorithm to solve the optimization and demonstrate its general applicability to common causal adjustment methods in § 4.

3.1 The parametric modeling approach to ATE estimation

We begin with estimating the ATE assuming oracle access to noiseless data $D^* = (X, Y, Z)$.¹ The ATE is identifiable given D^* due to [Assumption 1](#).

We adopt a parametric modeling approach to ATE estimation, where we posit a parametric model for the joint distribution $p_{x,y,z}$ or its components required by the identification formula. Specifically, we first posit a parametric model for the joint distribution or its relevant conditionals. For example, we may posit

¹The dataset contains n i.i.d. data points $\{X_i, Y_i, Z_i\}_{i=1}^n$. We suppress the data index for notation simplicity.

that the joint distribution $p_{x,y,z}$ follows a parametric model $\{p_\theta(x, y, z) : \theta \in \Theta\}$, where Θ is the parameter space. As another example, one may posit a parametric model only for a conditional component of $p_{x,y,z}$, e.g. $p_\theta(x, y, z) = p_x \times p_\theta(z|x) \times p_{y|x,z}$, where the conditional $p_{z|x}$ follows a statistical model parameterized by θ , $\{p_\theta(z|x) : \theta \in \Theta\}$. Given the parametric model, we find the likelihood maximizing parameter θ

$$\hat{\theta} = \arg \max_{\theta} L_n(\theta; p_{x,y,z}), \quad (4)$$

where $L_n(\theta; p_{x,y,z}) \triangleq \mathbb{E}_{p_{x,y,z}}[\log p_\theta(x, y, z)]$ is the likelihood of the data $D^* = (X, Y, Z)$ at parameter θ . Finally, we plug in the fitted parametric model for causal estimation

$$\hat{\tau} = Q(p_{\hat{\theta}}(x, y, z)), \quad (5)$$

where $p_{\hat{\theta}}(x, y, z)$ is the joint distribution of (X, Y, Z) implied by the posited statistical model at the optimal parameter $\hat{\theta}$, and $Q(\cdot)$ is the causal identification functional mapping the joint distribution of (X, Y, Z) to the ATE τ .

As an example, suppose we adopt the backdoor adjustment for estimation. We first posit a parametric model for $p_{y|x,z}$ with density $p_\theta(y|x, z) = \mathcal{N}(f(x, z; \theta), 1^2)$, find the maximum likelihood parameters $\hat{\theta}$ by maximizing $L_n(\theta; D^*)$, the Gaussian likelihood of the n data points in D^* given parameter θ , and finally calculate the ATE estimate following the backdoor adjustment $\hat{\tau} = \mathbb{E}_X[f(X, 1; \hat{\theta})] - \mathbb{E}_X[f(X, 0; \hat{\theta})]$.

3.2 Partial identification as robust optimization

The parametric approach to ATE estimation relies on having access to noiseless covariates X . However, we often only have access to the dataset with noisy covariates $D = (\tilde{X}, Y, Z)$, and the ATE is no longer point identifiable; they may only partially identify the ATE. Then how can we extend the parametric approach to partially identify the ATE?

Partial identification of ATE as a robust optimization. To perform partial identification, we extend the optimization problem of Eq. 4 to a robust optimization. The key observation is that, though the noiseless data distribution $p_{x,y,z}$ is unobserved, the observed noisy data distribution $p_{\tilde{x},y,z}$, together with the noise-level assumption (Assumption 2), characterizes an uncertainty set of $p_{x,y,z}$, which further leads to an uncertainty set of ATE, following the same identification formula in Eq. 5. If the uncertainty set of $p_{x,y,z}$ contains the true $p_{x,y,z}$, then its resulting uncertainty set for the ATE shall also contain the true ATE. In other words, the maximum and minimum of this ATE uncertainty set bound the true ATE, hence partial identification.

Formally, we obtain the partial identification interval by solving the following optimization problem analogous to the one in the parametric approach (Eqs. 4 and 5). Denote the uncertainty set of $p_{x,y,z}$ as $\mathcal{P}_{X,Y,Z}$. Then the lower bound of ATE $\hat{\tau}_L$ is obtained by

$$\hat{\tau}_L = \min_{p_{x,y,z} \in \mathcal{P}_{X,Y,Z}} Q(p_{\hat{\theta}}(x, y, z)) \quad (6)$$

$$\text{s.t. } \hat{\theta} = \arg \max_{\theta} L_n(\theta; p_{x,y,z}), \quad (7)$$

which is a form of a distributionally robust optimization (DRO). We can similarly obtain the upper bound $\hat{\tau}_U$ by replacing min with max, and the partial identification interval estimate for the ATE τ is $[\hat{\tau}_L, \hat{\tau}_U]$. It is similar to Eqs. 4 and 5: the parametric model is similarly placed on the noiseless data $p_{x,y,z}$. The only difference is that $p_{x,y,z}$ is unobserved; we have to calculate Eqs. 4 and 5 for all possible $p_{x,y,z}$ within the uncertainty set $\mathcal{P}_{X,Y,Z}$. This formulation of partial identification as robust optimization produces tight partial identification bounds. The tightness is achieved by construction, as any $p_{x,y,z}$ that achieves the minimum

and maximum value of the objective is compatible with the observed data and the posited statistical model due to the constraint of $p_{x,y,z} \in \mathcal{P}_{X,Y,Z}$. Below we discuss some practical aspects of partial identification: constructing the uncertainty set, solving the robust optimization problem, and statistical inference of the partial identification bounds.

The uncertainty set $\mathcal{P}_{X,Y,Z}$. To construct the uncertainty set of $p_{x,y,z}$, we focus on characterizing $p_{x|y,z}$, the conditional distribution of the noiseless covariates X given Y, Z . The reason is that the conditional distribution $p_{x|y,z}$, along with treatment and outcome distribution $p_{y,z}$, fully determines the joint $p_{x,y,z} = p_{x|y,z} \times p_{y,z}$. Thus the ATE can be identified by Eq. 5 under Assumption 1.

To construct the uncertainty set for $p_{x|y,z}$, we resort to Assumption 2, which requires that $p_{x|z} \in \{\bar{p}_{x|z} : \text{TV}(\bar{p}_{x|z}, p_{\bar{x}|z}) \leq \gamma_z\}$ for $z \in \{0, 1\}$. Let us denote $\gamma = (\gamma_z)_{z \in \{0,1\}}$. Thus, by the chain rule, the uncertainty set of $p_{x,y,z}$ is

$$\mathcal{P}_{X,Y,Z}(p_{\bar{x},y,z}; \gamma) = \left\{ p_{y,z} \times \bar{p}_{x|y,z} : \text{TV} \left(\int \bar{p}_{x|y,z} \times p_{y|z} dy, p_{\bar{x}|z} \right) \leq \gamma_z, \forall y \in \mathcal{Y}, z \in \{0, 1\} \right\}.$$

Solving the robust optimization problem. Eqs. 6 and 7 define a distributionally robust optimization (DRO) problem, which generally takes the form of a minimax optimization, $\min_{\theta \in \Theta} \max_{q: D(q,p) \leq \gamma} \mathbb{E}_{X,Y \sim q} [l(\theta, X, Y)]$, where D is some divergence metric between the distributions p and q , and $l : \Theta \times \mathcal{X} \times \mathcal{Y} \rightarrow \mathbb{R}$ (Duchi and Namkoong, 2018). Such problems can be solved by re-writing Eqs. 6 and 7 using via a Lagrangian formulation:

$$\hat{\tau}_L = \min_{\theta} \min_{p_{x,y,z} \in \mathcal{P}_{X,Y,Z}(p_{\bar{x},y,z}; \gamma)} \max_{\lambda \geq 0} Q(p_{\theta}(x, y, z)) - \lambda \cdot L_n(\theta; p_{x,y,z}), \quad (8)$$

when the function $L_n(\cdot)$ is upper bounded. We can then apply existing methods that efficiently and optimally solve the DRO problem different divergence metrics D (Namkoong and Duchi, 2016; Li et al., 2019; Esfahani and Kuhn., 2018), equipped with finite-sample convergence rates analyzed in Duchi and Namkoong (2018). (See Appendix A for details.)

Statistical inference of the partial identification bounds. The robust optimization problem (Eqs. 6 and 7) produces point estimates for the partial identification bounds of ATE. To assess the sampling uncertainty of these bounds, one can invoke standard statistical inference tools (Duchi and Namkoong, 2018). Specifically, we consider a separate TV ball around the observed data distribution $\{\bar{p}_{\bar{x},y,z} : \text{TV}(\bar{p}_{\bar{x},y,z}, p_{\bar{x},y,z}) \leq \rho/n\}$, where n is the sample size and $\rho = \chi_{1,1-\alpha}^2$ is the $(1 - \alpha)$ -quantile of the χ_1^2 distribution. We can then obtain upper and lower confidence limits for $\hat{\tau}_L$ and $\hat{\tau}_U$. For instance, for the lower bound of ATE $\hat{\tau}_L$, its upper and lower confidence limits are

$$u_{\hat{\tau}_L} = \min_{\theta} \min_{p_{x,y,z} \in \mathcal{P}_{X,Y,Z}(\bar{p}_{\bar{x},y,z}; \gamma)} \max_{\substack{\text{TV}(\bar{p}_{\bar{x},y,z}, p_{\bar{x},y,z}) \\ \leq \rho/n}} \max_{\lambda \geq 0} Q(p_{\theta}(x, y, z)) - \lambda \cdot L_n(\theta; p_{x,y,z}),$$

$$l_{\hat{\tau}_L} = \min_{\theta} \min_{p_{x,y,z} \in \mathcal{P}_{X,Y,Z}(\bar{p}_{\bar{x},y,z}; \gamma)} \min_{\substack{\text{TV}(\bar{p}_{\bar{x},y,z}, p_{\bar{x},y,z}) \\ \leq \rho/n}} \max_{\lambda \geq 0} Q(p_{\theta}(x, y, z)) - \lambda \cdot L_n(\theta; p_{x,y,z}).$$

Similarly, one can obtain the upper and low confidence limits of the upper bound $\hat{\tau}_U$. Importantly, these confidence limits $[l_{\hat{\tau}_L}, u_{\hat{\tau}_L}]$ quantify the sampling uncertainty of $\hat{\tau}_L$ because we do not have access to the true distribution $p_{\bar{x},y,z}$. In contrast, the partial identification bounds $[\hat{\tau}_L, \hat{\tau}_U]$ quantify the identification uncertainty of τ due to noisy covariates. As the sample size n increases, the confidence intervals $[l_{\hat{\tau}_L}, u_{\hat{\tau}_L}]$ and $[l_{\hat{\tau}_U}, u_{\hat{\tau}_U}]$ shrink to a point mass, but the identification interval $[\hat{\tau}_L, \hat{\tau}_U]$ does not shrink.

In more detail, suppose the propensity score given all observed covariates is $e(X_{\text{inc}}) \triangleq P(Z = 1 | X_{\text{inc}})$, where X_{inc} denotes all the observed covariates, which may not include all confounders and satisfy weak unconfoundedness (Imbens and Rubin, 2015). Further denote the propensity score given all confounders $e(X_{\text{full}}) \triangleq P(Z = 1 | X_{\text{full}})$, where X_{full} satisfy weak unconfoundedness $Z \perp Y(1), Y(0) | X_{\text{full}}$. Then the robust optimization approach to partial identification can be used to obtain ATE bounds under the sensitivity assumptions like $\text{TV}(p_{e(x_{\text{inc}})}, p_{e(x_{\text{full}})}) \leq \gamma$ or $\text{TV}(p_{e(x_{\text{inc}})|z}, p_{e(x_{\text{full}})|z}) \leq \gamma_z$ for some constants γ_z, γ .

4 Applications to Common Causal Adjustment Methods

In this section, we apply the general robust optimization strategy to a variety of popular causal adjustment methods. In particular, we instantiate the estimator (Eq. 6) for three adjustment methods, backdoor adjustment, inverse propensity weighting (IPW), and frontdoor adjustment. (We further demonstrate the application to double machine learning in Appendix B.) For each adjustment method, we first provide a brief review of the standard procedure, then demonstrate how it can be augmented to perform partial identification given noisy covariates. Specifically, we write the objective $Q(\cdot)$ and the likelihood constraint $L_n(\cdot)$ as a functional of the unobserved conditional $p_{x|y,z}$, because the uncertainty set of the joint $p_{x,y,z}$ is expressed in terms of $p_{x|y,z}$. These steps will enable us to solve the robust optimization problem by searching $p_{x|y,z}$ over the uncertainty set.

Backdoor adjustment. Under the backdoor criterion, backdoor adjustment estimates the potential outcomes $\mathbb{E}[Y(z)], z \in \{0, 1\}$ by $\mathbb{E}[Y(z)] = \int \mathbb{E}[Y|Z = z, X = x]P(X = x)dx$. If we had access to the noiseless covariates X , we estimate the ATE by positing a parametric model $\mathbb{E}[Y|Z = z, X = x] = g(x, z; \theta)$ and calculating $\hat{\tau} = \mathbb{E}[g(X, Z = 1; \theta) - g(X, Z = 0; \theta)]$.

Next we move from noiseless covariates to noisy ones. Given each feasible $p_{x|y,z}$, we inherit the identification formula as the optimization objective $Q(p_{\hat{\theta}}(x, y, z)) = \mathbb{E}_{p_{x|z=1}}[g(X, Z = 1; \theta)] - \mathbb{E}_{p_{x|z=0}}[g(X, Z = 0; \theta)]$, where $p_{x|z} = \int p_{x|y,z} \times p_{y|z} dy$. Then the constraint is that θ maximizes the expected log-likelihood given the dataset: $L_n(\theta; p_{x,y,z}) = \mathbb{E}_{Y,Z}[\mathbb{E}_{p_{x|y,z}}[\ell(f(X, Z; \theta), Y)]]$.

Inverse propensity weighting (IPW). The application to the IPW method share a similar spirit as backdoor adjustment except that IPW estimates the potential outcome $Y(z), z \in \{0, 1\}$ with a different estimator $\mathbb{E}[Y(z)] = \mathbb{E}[\frac{YZ}{P(Z=z|X)}]$. We estimate the ATE by positing a parametric model on the propensity score, $Z|X \sim \text{Bern}(f(\theta, X))$. Thus for each feasible $p_{x|y,z}$, we can estimate the ATE by $Q(p_{\hat{\theta}}(x, y, z)) = \mathbb{E}_{p_{y,z}} \mathbb{E}_{p_{x|y,z}}[\frac{YZ}{f(X;\theta)} - \frac{Y(1-Z)}{1-f(X;\theta)}]$, which is also the objective of the robust optimization problem. Then the constraint of this problem is that θ maximizes the likelihood of $p_{z|x}$, i.e. $L_n(\theta; p_{x,y,z}) = \mathbb{E}_z[\mathbb{E}_{p_{x|z}}[\text{Bern}(Z; f(X; \theta))]]$ with $p_{x|z} = \int p_{x|y,z} \times p_{y|z} dy$.

Frontdoor adjustment. Frontdoor adjustment is different from the backdoor adjustment and IPW in that the covariates X serve as mediators between the treatment Z and outcome Y . Frontdoor adjustment gives the following estimator for potential outcomes, $\mathbb{E}[Y(z)] = \mathbb{E}_{X \sim P(X|Z=z)}[\sum_{z'=0,1} \mathbb{E}[Y|X, Z = z']P(Z = z')]$. Similar to backdoor adjustment, we can parameterize $\mathbb{E}[Y|X = x, Z = z] = g(x, z; \theta)$. Thus the ATE identification functional is $Q(p_{\hat{\theta}}(x, y, z)) = \mathbb{E}_{X \sim P(X|Z=1)}[\sum_{z'=0,1} g(X, z'; \theta)P(Z = z')] - \mathbb{E}_{X \sim P(X|Z=0)}[\sum_{z'=0,1} g(X, z'; \theta)P(Z = z')]$. As we use the same parametric model as in backdoor adjustment, the constraint of the robust optimization problem of the frontdoor adjustment is the same as that of the backdoor adjustment, where $L_n(\theta; p_{x,y,z}) = \mathbb{E}_{Y,Z}[\mathbb{E}_{p_{x|y,z}}[\ell(f(X, Z; \theta), Y)]]$.

5 Experiments

We empirically evaluate the performance of the partial identification for noisy covariates via robust optimization (abbreviated as RCI) on a variety of simulated and real datasets. For each dataset, we synthetically generate noisy versions of it with different noise levels. For each noise level, we compute the noise strength γ_z as the TV distance in Eq. 2, which is a parameter of RCI to estimate ATE. We study the performance of RCI applied to a variety of standard causal estimators, including the backdoor adjustment estimator, the IPW estimator and the frontdoor adjustment, comparing them with a naive approach that employs the corresponding estimator directly applied to the noisy data. We find that RCI provides partial identification intervals with improved coverage properties than existing approaches, including the Causal Effect Variational Autoencoder (CEVAE) (Louizos et al., 2017), while being not overly conservative (e.g. Fig. 1). We provide the details of the datasets, evaluation procedures and results in sequel. Further data and training details are in Appendix C.

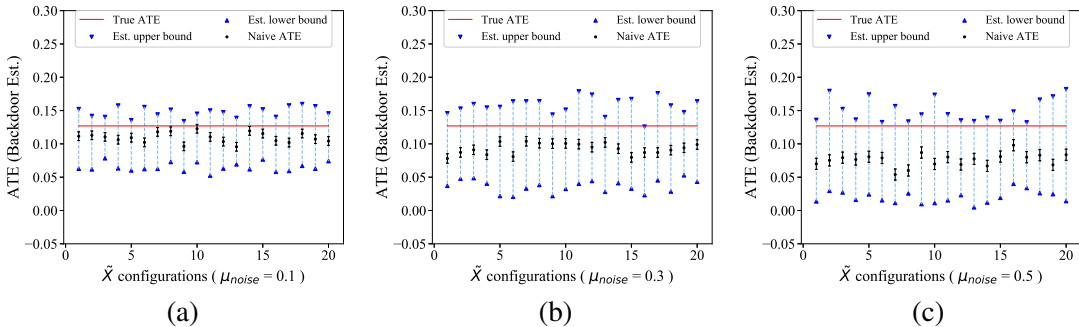


Figure 1: Partial identification of ATE with backdoor adjustment estimators on synthetic dataset with binary outcome. The three noise levels have random Gaussian noise with mean = 0.1/0.3/0.5 and standard deviation = 0.5/0.5/1. In all plots, we compare RCI (this work) to the naive approach. The error bars indicate 95% confidence interval of the naive ATE estimation over twenty trials. *Intervals covering the true ATE is better.*

5.1 Synthetic data

Backdoor adjustment and IPW. To evaluate the performance of the robust approach with the backdoor adjustment and IPW estimators, we synthetically generate two datasets with X as the confounder. To demonstrate the variability of the estimated ATE intervals, we first synthetically generate a dataset with binary outcomes according to a logistic model. We further consider another synthetic dataset with a more complicated nonlinear outcome model and continuous outcomes, using the Kang and Schafer example (Kang et al., 2007), which consists of four unobserved covariates $U_i \stackrel{iid}{\sim} N(0, I_4)$, $i = 1, \dots, n$. The full data generation details are included in Appendix C.1.

Frontdoor adjustment. For front adjustment, we synthetically generate two datasets, with X as the mediators. First, we generate a dataset with binary outcomes using a logistic model with a single mediator. We then generate another more complicated using a similar data generation as in Jung et al. (2020). This data generation is more complicated with multiple mediators.

Noisy data generation. Given the true covariates, we generate noisy covariates by synthetically adding a small amount of random noise. The ground truth covariates enables us to estimate the true ATE. For each selected example, we perturb it by adding a noise drawn from a Gaussian distribution to each dimension.

Table 1: Coverage probabilities for the partial identification interval via robust optimization with the backdoor adjustment and IPW estimators, and the naive approach and CEVAE (averaged over 100 trials, with standard error). (*higher is better*).

Noise	Naive	CEVAE	RCI	
			Backdoor Adj.	IPW
level 1	0.10 ± 0.09	0.46 ± 0.17	1.00 ± 0.00	0.95 ± 0.02
level 2	0.00 ± 0.00	0.41 ± 0.05	0.98 ± 0.01	0.93 ± 0.03
level 3	0.00 ± 0.00	0.42 ± 0.09	0.97 ± 0.02	0.91 ± 0.03
level 4	0.00 ± 0.00	0.33 ± 0.03	0.95 ± 0.02	0.87 ± 0.03
level 5	0.00 ± 0.00	0.32 ± 0.14	0.93 ± 0.03	0.85 ± 0.04

Table 2: Coverage probabilities for the robust optimization approach with frontdoor adjustment, and the naive approach. (a) shows results with simulation data contains multiple mediators (mean and standard errors are averaged over 100 trials.). (b) shows results with the IHDP dataset (mean and standard errors are averaged over 50 trials.) (*higher is better*).

Noise	Naive	RCI (Frontdoor)	Noise	Naive	RCI (Frontdoor)
level 1	0.30 ± 0.15	0.92 ± 0.03	level 1	0.30 ± 0.15	0.98 ± 0.02
level 2	0.10 ± 0.09	0.87 ± 0.03	level 2	0.10 ± 0.09	0.96 ± 0.03
level 3	0.00 ± 0.00	0.84 ± 0.04	level 3	0.00 ± 0.00	0.94 ± 0.04
level 4	0.00 ± 0.00	0.82 ± 0.04	level 4	0.00 ± 0.00	0.94 ± 0.04
level 5	0.00 ± 0.00	0.81 ± 0.04	level 5	0.00 ± 0.00	0.92 ± 0.04

We then evaluate the performance of the different algorithms ranging from small to large amounts of noise. The full generation details are in C.1.

Evaluation and results. To demonstrate the variability of the estimated ATE intervals, we plot the ATE intervals obtained by RCI and the true ATE. As a comparison, we also show the results of the naive ATE estimator, which estimates ATE directly using the noisy examples. The true ATE is calculated using the corresponding adjustment method and the noiseless covariates. We generate 2000 samples for each adjustment method, and generate 20 configurations of the noisy covariates for each noise level.

Figure 1 shows the performance of different algorithms using the backdoor adjustment method. The results with frontdoor adjustment method are similar and included in Appendix C.5. We observe that under the two outcome models, RCI can provide ATE intervals with a high coverage on the true ATE. However, the naive approach is very sensitive to the noise even for the low noise levels, and gives estimations that deviate from the true ATE as the noise level increases. Moreover, the RCI intervals are not overly conservative or trivial: they cover the true ATE without much overshooting. We compute the true ATE coverage probability with the more complicated Kang and Schafer example (used for backdoor adjustment and IPW), and the second simulated dataset with multiple mediators for the frontdoor adjustment method. We also compare with CEVAE (Louizos et al., 2017), which identifies ATE via back-door adjustment and models the noised covariates as the proxy variables. A success cover means that the true ATE is contained in the estimated ATE interval by RCI, or by the 95% confidence intervals of naive ATE. For CEVAE, at a specific noise level, we collect its ATE estimates over multiple datasets with noisy covariates. A success cover means the true ATE is within the range of estimates from the noisy datasets. We generate ten random noiseless datasets of

Table 3: Coverage probabilities for the robust optimization approach with the backdoor adjustment and IPW estimators, and the naive approach, using the ACIC dataset. (The results are averaged over 50 trials). (*higher is better*).

Noise	Naive	CEVAE	RCI	
			Backdoor Adj.	IPW
level 1	0.02 ± 0.02	0.81 ± 0.07	1.00 ± 0.00	1.00 ± 0.00
level 2	0.00 ± 0.00	0.73 ± 0.05	0.98 ± 0.02	0.98 ± 0.02
level 3	0.00 ± 0.00	0.75 ± 0.10	0.94 ± 0.03	0.92 ± 0.04
level 4	0.00 ± 0.00	0.64 ± 0.02	0.94 ± 0.03	0.90 ± 0.04
level 5	0.00 ± 0.00	0.64 ± 0.03	0.90 ± 0.04	0.90 ± 0.04

true covariates with size 2000. For each noiseless dataset, we further generate ten equal-sized datasets with noisy covariates by drawing fresh noise samples. Therefore, the coverage probabilities are calculated over 100 pairs of true and noisy datasets. Table 1 and Table 2 (*left*) show the coverage probabilities using the three adjustment methods. We see that RCI is able to maintain a much higher coverage probability as the noise level increases.

5.2 Real data case studies

We further test the robust approach RCI on two case studies with real covariates, including an ACIC dataset and an IHDP dataset. Both datasets have been used for benchmarking various causal inference algorithms (Shalit et al., 2017; Shi et al., 2019; Gupta et al., 2020).

Case study 1: ACIC dataset. We first use a dataset constructed for the Atlantic Causal Inference Conference (ACIC) 2019 Data Challenge based on the “spambase” dataset for spam email detection from UCI (Gruber et al., 2019; Dua and Graff, 2017). This dataset consists of emails with an outcome of interest Y being whether or not the email was marked as spam by a user. The treatment Z represents whether or not the email contains more than a given threshold of capital letters, where this threshold is computed by a mean over the original dataset. There are 22 continuous covariates X which are word frequencies given as percentages between 0 and 100. We generate our dataset directly using ACIC’s data generating process, with a size of 2000 examples. Given the true covariates, we further generate noisy covariates by synthetically adding a small amount of noise at random, using a similar procedure as for the synthetic data. Specifically, we generate five levels of Gaussian noise with mean = 0.1/0.2/0.3/0.4/0.5 and standard deviations at 0.5/0.5/1/1/1.

Case study 2: IHDP dataset. For a second case study, we use a benchmark dataset introduced by Hill (2011), which is constructed from data obtained from the Infant Health and Development Program (IHDP). This dataset is based on a randomized experiment to measure the effect of home visits from a specialist on future test scores of children. The confounders U correspond to collected measurements of the children and their mothers used during a randomized experiment that studied the effect of home visits by specialists on future cognitive test scores. We use samples from the NPCI package (Dorie, 2016), which converted the randomized data to an observational study by removing a biased subset of the treated group. The final dataset contains 747 samples with 25 covariates. We then simulate the mediator and the outcome using a procedure similar to Hill (2011); Gupta et al. (2020). We generated the noisy covariates using the same five noise levels as the ACIC dataset. The full generation details are in C.4.

Evaluation results. We evaluated the naive approach, the RCI approach with the backdoor adjustment and

IPW adjustment methods on the ACIC dataset. We also evaluated the naive approach and RCI with the frontdoor adjustment method on the IHDP dataset. Table 3 and Table 2(right) show the coverage probabilities using these three adjustment methods. For both case studies, RCI is able to maintain a much higher coverage probability as the noise level increases, while the naive approach’s estimates turn out to be very sensitive to the noise and have low coverage probabilities. Frontdoor adjustment method is able to achieve a higher coverage probability comparing to the synthetic data. This could be due to the fact that, in this data generation model, the outcome is linearly correlated with the mediator. As we also used a linear parameterized model, there is no model specification.

6 Conclusion

This paper develops an approach to partial identification for noisy covariates via robust optimization. We show that partial identification can be formulated as a robust optimization problem, which enables bounds on causal effects for parametric causal models. We then derive a variant of the projected gradient algorithm to efficiently solve the robust optimization problem and compute partial identification bounds on the causal effect of interest. We illustrate the wide applicability of our approach on a variety of causal adjustment methods, including the backdoor adjustment, inverse propensity weighting and the frontdoor adjustment. Numerical results across synthetic and real-world data show that this approach can effectively compute bounds for ATE with higher coverage than previous methods without being overly conservative.

Acknowledgements

The authors would like to thank Peng Ding for extensive discussions and helpful suggestions that significantly improved the paper. The authors also thank Peter Bickel, Avi Feller, Sam Pimentel, Vira Semenova, and Yan Shuo Tan for helpful feedback on early versions of the paper. This work was supported in part by the Mathematical Data Science program of the Office of Naval Research under grant number N00014-18-1-2764. WG acknowledges support from a Google PhD fellowship; MY acknowledges support from the Irving Institute for Cancer Dynamics.

References

- Alexander Balke and Judea Pearl. Counterfactual probabilities: Computational methods, bounds and applications. In *Uncertainty Proceedings 1994*, pages 46–54. Elsevier, 1994.
- Alexander Balke and Judea Pearl. Bounds on treatment effects from studies with imperfect compliance. *Journal of the American Statistical Association*, 92(439):1171–1176, 1997.
- Arindam Banerjee, Srujana Merugu, Inderjit S Dhillon, Joydeep Ghosh, and John Lafferty. Clustering with bregman divergences. *Journal of machine learning research*, 6(10), 2005.
- Mohamed Ishmael Belghazi, Aristide Baratin, Sai Rajeshwar, Sherjil Ozair, Yoshua Bengio, Aaron Courville, and Devon Hjelm. Mutual information neural estimation. In *International Conference on Machine Learning*, pages 531–540. PMLR, 2018.
- Aharon Ben-Tal, Laurent El Ghaoui, and Arkadi Nemirovski. *Robust Optimization*. Princeton Series in Applied Mathematics. Princeton University Press, October 2009.

- Dimitris Bertsimas, David B Brown, and Constantine Caramanis. Theory and applications of robust optimization. *SIAM Review*, 53(3):464–501, 2011.
- Blai Bonet. Instrumentality tests revisited. *arXiv preprint arXiv:1301.2258*, 2013.
- Matteo Bonvini and Edward H Kennedy. Sensitivity analysis via the proportion of unmeasured confounding. *Journal of the American Statistical Association*, pages 1–31, 2020.
- David Card. The causal effect of education on earnings. In *Handbook of Labor Economics*, volume 3, pages 1801–1863. Elsevier, 1999.
- Raymond J Carroll, David Ruppert, Leonard A Stefanski, and Ciprian M Crainiceanu. *Measurement error in nonlinear models: a modern perspective*. CRC press, 2006.
- Victor Chernozhukov, Denis Chetverikov, Mert Demirer, Esther Duflo, Christian Hansen, Whitney Newey, and James Robins. Double/debiased machine learning for treatment and structural parameters, 2018.
- Carlos Cinelli and Chad Hazlett. Making sense of sensitivity: Extending omitted variable bias. *Journal of the Royal Statistical Society: Series B (Statistical Methodology)*, 82(1):39–67, 2020.
- Carlos Cinelli, Daniel Kumor, Bryant Chen, Judea Pearl, and Elias Bareinboim. Sensitivity analysis of linear structural causal models. In *International Conference on Machine Learning (ICML)*, pages 1252–1261. PMLR, 2019.
- Alfred F Connors, Theodore Speroff, Neal V Dawson, Charles Thomas, Frank E Harrell, Douglas Wagner, Norman Desbiens, Lee Goldman, Albert W Wu, Robert M Califf, et al. The effectiveness of right heart catheterization in the initial care of critically ill patients. *Journal of the American Medical Association*, 276(11):889–897, 1996.
- Yifan Cui, Hongming Pu, Xu Shi, Wang Miao, and Eric Tchetgen Tchetgen. Semiparametric proximal causal inference. *arXiv preprint arXiv:2011.08411*, 2020.
- V. Dorie. Non-parametrics for causal inference. <https://github.com/vdorie/npci>, 2016.
- Vincent Dorie, Masataka Harada, Nicole Bohme Carnegie, and Jennifer Hill. A flexible, interpretable framework for assessing sensitivity to unmeasured confounding. *Statistics in Medicine*, 35(20):3453–3470, 2016.
- Dheeru Dua and Casey Graff. UCI machine learning repository, 2017. URL <http://archive.ics.uci.edu/ml>.
- Guilherme Duarte, Noam Finkelstein, Dean Knox, Jonathan Mummolo, and Ilya Shpitser. An automated approach to causal inference in discrete settings. *arXiv preprint arXiv:2109.13471*, 2021.
- John Duchi and Hongseok Namkoong. Learning models with uniform performance via distributionally robust optimization. *arXiv preprint arXiv:1810.08750*, 2018.
- John Duchi, Shai Shalev-Shwartz, Yoram Singer, and Tushar Chandra. Efficient projections onto the l_1 -ball for learning in high dimensions. In *International Conference on Machine Learning (ICML)*, pages 272–279, 2008.

- Oliver Dukes, Ilya Shpitser, and Eric J Tchetgen Tchetgen. Proximal mediation analysis. *arXiv preprint arXiv:2109.11904*, 2021.
- P. M. Esfahani and D. Kuhn. Data-driven distributionally robust optimization using the Wasserstein metric: Performance guarantees and tractable reformulations. *Mathematical Programming*, 171:115–166, 2018.
- Noam Finkelstein, Roy Adams, Suchi Saria, and Ilya Shpitser. Partial identifiability in discrete data with measurement error. *arXiv preprint arXiv:2012.12449*, 2020.
- AlexanderM Franks, Alexander D’Amour, and Avi Feller. Flexible sensitivity analysis for observational studies without observable implications. *Journal of the American Statistical Association*, 2019.
- Peter A Frost. Proxy variables and specification bias. *The Review of Economics and Statistics*, pages 323–325, 1979.
- Wayne A Fuller. *Measurement error models*, volume 305. John Wiley & Sons, 2009.
- Dan Geiger and Christopher Meek. Quantifier elimination for statistical problems. In *Proceedings of the Fifteenth conference on Uncertainty in artificial intelligence*, pages 226–235, 1999.
- Susan Gruber, Geneviève Lefebvre, Tibor Schuster, and Alexandre Piché. Atlantic causal inference conference data challenge, 2019. URL <https://sites.google.com/view/acic2019datachallenge/>.
- Shantanu Gupta, Zachary C Lipton, and David Childers. Estimating treatment effects with observed confounders and mediators. *arXiv preprint arXiv:2003.11991*, 2020.
- Jan-Eric Gustafsson. Causal inference in educational effectiveness research: A comparison of three methods to investigate effects of homework on student achievement. *School Effectiveness and School Improvement*, 24(3):275–295, 2013.
- James J Heckman and Edward J Vytlacil. Instrumental variables, selection models, and tight bounds on the average treatment effect. In *Econometric Evaluation of Labour Market Policies*, pages 1–15. Springer, 2001.
- Jennifer L Hill. Bayesian nonparametric modeling for causal inference. *Journal of Computational and Graphical Statistics*, 20(1):217–240, 2011.
- Jesse Y Hsu and Dylan S Small. Calibrating sensitivity analyses to observed covariates in observational studies. *Biometrics*, 69(4):803–811, 2013.
- Kosuke Imai and Teppei Yamamoto. Causal inference with differential measurement error: Nonparametric identification and sensitivity analysis. *American Journal of Political Science*, 54(2):543–560, 2010.
- Guido W Imbens. Sensitivity to exogeneity assumptions in program evaluation. *American Economic Review*, 93(2):126–132, 2003.
- Guido W Imbens and Donald B Rubin. *Causal inference in statistics, social, and biomedical sciences*. Cambridge University Press, 2015.
- Yonghan Jung, Jin Tian, and Elias Bareinboim. Estimating causal effects using weighting-based estimators. In *AAAI Conference on Artificial Intelligence*, volume 34, pages 10186–10193, 2020.

- Nathan Kallus, Xiaojie Mao, and Madeleine Udell. Causal inference with noisy and missing covariates via matrix factorization. In *Advances in Neural Information Processing Systems (NeurIPS)*, pages 6921–6932, 2018.
- Joseph DY Kang, Joseph L Schafer, et al. Demystifying double robustness: A comparison of alternative strategies for estimating a population mean from incomplete data. *Statistical Science*, 22(4):523–539, 2007.
- Manabu Kuroki and Judea Pearl. Measurement bias and effect restoration in causal inference. *Biometrika*, 101(2):423–437, 2014.
- Jiajin Li, Sen Huang, and Anthony Man-Cho So. A first-order algorithmic framework for Wasserstein distributionally robust logistic regression. In *Advances in Neural Information Processing Systems (NeurIPS)*, 2019.
- Weiwei Liu, S Janet Kuramoto, and Elizabeth A Stuart. An introduction to sensitivity analysis for unobserved confounding in nonexperimental prevention research. *Prevention Science*, 14(6):570–580, 2013.
- JR Lockwood and Daniel F McCaffrey. Matching and weighting with functions of error-prone covariates for causal inference. *Journal of the American Statistical Association*, 111(516):1831–1839, 2016.
- Christos Louizos, Uri Shalit, Joris M Mooij, David Sontag, Richard Zemel, and Max Welling. Causal effect inference with deep latent-variable models. In *Advances in Neural Information Processing Systems (NeurIPS)*, pages 6446–6456, 2017.
- Lester Mackey, Vasilis Syrgkanis, and Ilias Zadik. Orthogonal machine learning: Power and limitations. In *International Conference on Machine Learning (ICML)*, pages 3375–3383. PMLR, 2018.
- Wang Miao, Zhi Geng, and Eric J Tchetgen Tchetgen. Identifying causal effects with proxy variables of an unmeasured confounder. *Biometrika*, 105(4):987–993, 2018.
- Hongseok Namkoong and John C Duchi. Stochastic gradient methods for distributionally robust optimization with f-divergences. In *Advances in Neural Information Processing Systems (NeurIPS)*, pages 2208–2216, 2016.
- Jerzy Neyman. Sur les applications de la thar des probabilités aux expériences agaricales: Essay des principe. excerpts reprinted (1990) in english. *Statistical Science*, 5(463-472):4, 1923.
- Elizabeth L Ogburn and Tyler J Vanderweele. Bias attenuation results for nondifferentially mismeasured ordinal and coarsened confounders. *Biometrika*, 100(1):241–248, 2013.
- Judea Pearl. Causal diagrams for empirical research. *Biometrika*, 82(4):669–688, 1995.
- Judea Pearl. *Causality*. Cambridge university press, 2009.
- Fernando Pérez-Cruz. Kullback-leibler divergence estimation of continuous distributions. In *2008 IEEE international symposium on information theory*, pages 1666–1670. IEEE, 2008.
- Roland R Ramsahai and Peter Spirtes. Causal bounds and observable constraints for non-deterministic models. *Journal of Machine Learning Research*, 13(3), 2012.

- Amy Richardson, Michael G Hudgens, Peter B Gilbert, and Jason P Fine. Nonparametric bounds and sensitivity analysis of treatment effects. *Statistical Science: A Review Journal of the Institute of Mathematical Statistics*, 29(4):596, 2014.
- Paul R Rosenbaum and Donald B Rubin. The central role of the propensity score in observational studies for causal effects. *Biometrika*, 70(1):41–55, 1983.
- Paul R Rosenbaum et al. *Design of Observational Studies*, volume 10. Springer, 2010.
- Donald B Rubin. Estimating causal effects of treatments in randomized and nonrandomized studies. *Journal of Educational Psychology*, 66(5):688, 1974.
- Michael C Sachs, Erin E Gabriel, and Arvid Sjölander. Symbolic computation of tight causal bounds. *arXiv preprint arXiv:2003.10702*, 2020.
- Susanne M Schennach. Recent advances in the measurement error literature. *Annual Review of Economics*, 8:341–377, 2016.
- Tobias Schnabel, Adith Swaminathan, Ashudeep Singh, Navin Chandak, and Thorsten Joachims. Recommendations as treatments: Debiasing learning and evaluation. *arXiv preprint arXiv:1602.05352*, 2016.
- Uri Shalit, Fredrik D Johansson, and David Sontag. Estimating individual treatment effect: generalization bounds and algorithms. In *International Conference on Machine Learning (ICML)*, pages 3076–3085. PMLR, 2017.
- Amit Sharma, Emre Kiciman, et al. Dowhy: A python package for causal inference. In *KDD 2019 workshop*, 2019.
- Changyu Shen, Xiaochun Li, Lingling Li, and Martin C Were. Sensitivity analysis for causal inference using inverse probability weighting. *Biometrical Journal*, 53(5):822–837, 2011.
- Claudia Shi, David M Blei, and Victor Veitch. Adapting neural networks for the estimation of treatment effects. *arXiv preprint arXiv:1906.02120*, 2019.
- Xu Shi, Wang Miao, Jennifer C Nelson, and Eric J Tchetgen Tchetgen. Multiply robust causal inference with double-negative control adjustment for categorical unmeasured confounding. *Journal of the Royal Statistical Society: Series B (Statistical Methodology)*, 82(2):521–540, 2020.
- Xu Shi, Wang Miao, Mengtong Hu, and Eric Tchetgen Tchetgen. On proximal causal inference with synthetic controls. *arXiv preprint arXiv:2108.13935*, 2021.
- Ilya Shpitser, Zach Wood-Doughty, and Eric J Tchetgen Tchetgen. The proximal id algorithm. *arXiv preprint arXiv:2108.06818*, 2021.
- Eric J Tchetgen Tchetgen, Andrew Ying, Yifan Cui, Xu Shi, and Wang Miao. An introduction to proximal causal learning. *arXiv preprint arXiv:2009.10982*, 2020.
- Victor Veitch and Anisha Zaveri. Sense and sensitivity analysis: Simple post-hoc analysis of bias due to unobserved confounding. *arXiv preprint arXiv:2003.01747*, 2020.
- Cédric Villani. *Optimal transport: old and new*, volume 338. Springer Science & Business Media, 2008.

- Yixin Wang, Dawen Liang, Laurent Charlin, and David M Blei. Causal inference for recommender systems. In *Fourteenth ACM Conference on Recommender Systems*, pages 426–431, 2020.
- Michael R Wickens. A note on the use of proxy variables. *Econometrica: Journal of the Econometric Society*, pages 759–761, 1972.
- Steve Yadlowsky, Hongseok Namkoong, Sanjay Basu, John Duchi, and Lu Tian. Bounds on the conditional and average treatment effect with unobserved confounding factors. *arXiv preprint arXiv:1808.09521*, 2018.
- Mingzhang Yin, Claudia Shi, Yixin Wang, and David M Blei. Conformal sensitivity analysis for individual treatment effects. *arXiv preprint arXiv:2112.03493*, 2021.
- Andrew Ying, Wang Miao, Xu Shi, and Eric J Tchetgen Tchetgen. Proximal causal inference for complex longitudinal studies. *arXiv preprint arXiv:2109.07030*, 2021.
- Junzhe Zhang and Elias Bareinboim. Bounding causal effects on continuous outcomes. 2021a.
- Junzhe Zhang and Elias Bareinboim. Non-parametric methods for partial identification of causal effects. Technical report, Technical Report Technical Report R-72, Columbia University, Department of ..., 2021b.
- Junzhe Zhang, Jin Tian, and Elias Bareinboim. Partial identification of counterfactual distributions. 2021.
- Qingyuan Zhao, Dylan S Small, and Bhaswar B Bhattacharya. Sensitivity analysis for inverse probability weighting estimators via the percentile bootstrap. *arXiv preprint arXiv:1711.11286*, 2017.

A Further Details about Solving the General DRO problem

In this section, we describe the details on solving the general DRO problem Eq. 6 with total variation (TV) distance using the empirical Lagrangian formulation.

Many existing works on DRO study how to solve the DRO problem for different divergence metrics D . The robust optimization problem (Eqs. 6 and 7) can be written in the form of a DRO problem with TV distance by Lagrangian formulation. Namkoong and Duchi (2016) provide methods for efficiently and optimally solving the DRO problem for f -divergences, and other work has provided methods for solving the DRO problem for Wasserstein distances (Li et al., 2019; Esfahani and Kuhn., 2018). Duchi and Namkoong (2018) further provide finite-sample convergence rates for the empirical version of the DRO problem.

Below we describe the empirical Lagrangian formulation and adopt a projected gradient-based algorithm to solve it and provide the pseudo-code of the algorithm.

A.1 Empirical Lagrangian formulation

In a general form, we consider the parameterized ATE estimator $\hat{\tau}$ as a general function of $\bar{p}_{x|y,z}$, $z \in \{0, 1\}$, $f_0(\bar{p}_{x|y,z=0}, \bar{p}_{x|y,z=1}; \theta)$, where θ denotes the parameters, and f_0 denotes the identification functional of ATE, e.g. the g -formula. We write f_0 as a functional of $p_{x|y,z}$ because, within the full joint $p_{x,y,z}$ that can enable ATE identification, $p_{x|y,z}$ is the only component that is unobserved.

For simplicity of exposition, we first consider a special case of the constraint in Eq. 7, i.e. when we assume independent Gaussian noise in the statistical model of $p_{x,y,z}$, e.g. $\bar{p}_\theta(x|y, z) = \mathcal{N}(h_{\theta_1}(y, z), \theta_2^2)$. In this case, the constraint in Eq. 7 becomes equivalent to minimizing the mean squared error (MSE). Denote the MSE as $f_1(\bar{p}_{x|y,z}; \theta)$. We then rewrite the constraint as $f_1(\bar{p}_{x|y,z}; \theta) \leq \epsilon$, where $\epsilon > 0$ is a slack variable taking on a small positive value.

Then Eqs. 6 and 7 becomes

$$\begin{aligned} \min_{\theta, \bar{p}_{x|y,z} \in \mathcal{P}_{X|Y,Z}, z=0,1} \quad & f_0(\bar{p}_{x|y,z=0}, \bar{p}_{x|y,z=1}; \theta) \\ \text{s.t.} \quad & f_1(\bar{p}_{x|y,z=0}, \bar{p}_{x|y,z=1}; \theta) \leq \epsilon \end{aligned} \tag{9}$$

For simplicity, let $v(\bar{p}_{x|y,z=0}; \theta) = f_1 - \epsilon$. Then the Lagrangian of Eq. 9 is:

$$L(\bar{p}_{x|y,z=0}, \bar{p}_{x|y,z=1}, \lambda; \theta) = f_0(\bar{p}_{x|y,z=0}, \bar{p}_{x|y,z=1}; \theta) + \langle \lambda, v(\bar{p}_{x|y,z=0}, \bar{p}_{x|y,z=1}; \theta) \rangle,$$

where $\lambda \geq 0$ is the Lagrange multiplier. Thus the optimization problem of Eq. 9 can be rewritten as

$$\min_{\theta \in \Theta} \min_{\bar{p}_{x|y,z} \in \mathcal{P}_{X|Y,Z}, z=0,1} \max_{\lambda \geq 0} L(\bar{p}_{x|y,z=0}, \bar{p}_{x|y,z=1}, \lambda; \theta). \tag{10}$$

It remains to solve Eq. 10, for which we resort to the empirical formulation of the DRO problem. Specifically, we replace all expectations with expectations over empirical distributions given a dataset of n samples, i.e. $D = \{(\tilde{X}_1, Y_1, Z_1), \dots, (\tilde{X}_n, Y_n, Z_n)\}$. Specifically, we consider the TV constraint between the respective empirical distributions of $\bar{p}_{x|z}$ and $p_{\tilde{x}|z}$, as opposed to their population version to which we do not have access. Such a TV constraint between empirical distributions reduces to an ℓ_1 norm constraint due to the definition of the TV distance. This ℓ_1 reduction is particular suitable for efficient solving the DRO problem, which we detail in Appendix A.2.

In more detail, for each $z \in \{0, 1\}$, let n_z be the number of samples with $Z_i = z$. Then we consider the empirical version of $p_{\tilde{x}|z} \in \mathbb{R}^{n_z \times |\tilde{\mathcal{X}}|}$ be a probability table with n_z rows and $|\tilde{\mathcal{X}}|$ columns, where $\tilde{\mathcal{X}}_z$ is set of (unique) values taken by $(\tilde{X}_i)_{Z_i=z}$; its (i, j) cell takes the value $p_{\tilde{x}|z}^i = \frac{1}{n_z}$ if the i -th example satisfies $Z_i = z$, X_i takes the j th value in the $\tilde{\mathcal{X}}_z$ set. We then consider the empirical distribution of $\bar{p}_{x|z} \in \mathbb{R}^{n_z}$ in a similar way and rewrite the TV distance constraint as ℓ_1 norm constraints: $\|\bar{p}_{x|z}, p_{\tilde{x}|z}\|_1 \leq 2\gamma_z$ for all $z \in \{0, 1\}$.

Replacing all expectations with expectations over the appropriate empirical distributions, we rewrite the constraints as ℓ_1 norm constraints on the empirical distribution of X given Z . Then Eq. 10 is equivalent to:

$$\begin{aligned} \min_{\theta} \max_{\lambda \geq 0} \max_{\substack{\bar{p}_{x|y,z=0}, \bar{p}_{x|y,z=1} \\ z=0,1}} L(\bar{p}_{x|y,z=0}, \bar{p}_{x|y,z=1}, \lambda; \theta) \\ \text{s.t. } \|\bar{p}_{x|z} - p_{\tilde{x}|z}\|_1 \leq 2\gamma_z, \quad \|\bar{p}_{x|z}\|_1 = 1, \quad \forall z \in \{0, 1\}. \end{aligned} \quad (11)$$

A.2 Projected GDA algorithm

To solve Eq. 11, we use a projected gradient descent ascent (GDA) algorithm, which is a simplified version of the algorithm introduced by Namkoong and Duchi (2016) for solving general classes of DRO problems. Note that projections onto an ℓ_1 -ball can be done efficiently (Duchi et al., 2008). We provide the pseudocode in Alg. 1. The implementation code will be made public.

Algorithm 1 Project GDA Algorithm for the general DRO formulation

Require: learning rates $\eta_\theta > 0, \eta_\lambda > 0, \eta_z > 0, z = 0, 1$; upper bounds $\gamma_z > 0, z = 0, 1$.

- 1: **for** $t = 1, \dots, T$ **do**
 - 2: *Descent step on θ :*
 Compute $\theta^{(t+1)} \leftarrow \theta^{(t)} - \eta_\theta \cdot \nabla_{\theta} L(\bar{p}_{x|y,z=0}^{(t)}, \bar{p}_{x|y,z=1}^{(t)}, \lambda^{(t)}; \theta^{(t)})$
 - 3: *Ascent step on λ :*
 Compute $\lambda^{(t+1)} \leftarrow \lambda^{(t)} + \eta_\lambda \cdot \mathbf{v}(\bar{p}_{x|y,z=0}^{(t)}, \bar{p}_{x|y,z=1}^{(t)}; \theta^{(t)})$
 - 4: **for** $z \in \{0, 1\}$ **do**
 - 5: *Ascent step on $\bar{p}_{x|z}$:* Compute $\bar{p}_{x|z}^{(t+1)} \leftarrow \bar{p}_{x|z}^{(t)} + \eta_z \cdot \nabla_{\bar{p}_{x|z}} L(\bar{p}_{x|z=0}^{(t)}, \bar{p}_{x|z=1}^{(t)}, \lambda^{(t)}; \theta^{(t)})$
 - 6: *Project $\bar{p}_{x|z}^{(t+1)}$ onto ℓ_1 -norm constraints:* $\|\bar{p}_{x|z}^{(t+1)} - p_{\tilde{x}|z}\|_1 \leq 2\gamma_z, \|\bar{p}_{x|z}^{(t+1)}\|_1 = 1$
 - 7: **end for**
 - 8: **end for**
 - 9: **return** $\theta^{(t^*)}$ and $\bar{p}_{x|z}^{(t^*)}, z = 0, 1$ where t^* denotes the *best* iterate that satisfies the constraints in (Eq. 11) with the lowest objective.
-

B Application to Double Machine Learning

In this section, we demonstrate how the robust optimization approach can also be applied to the double machine learning estimator (Chernozhukov et al., 2018). In particular, we use a partially linear model (PLM) as in Mackey et al. (2018).

Given i.i.d samples of (X, Y, Z) , double machine learning estimates ATE as

$$\hat{\tau} = \frac{\mathbb{E}[(Y - f(X; \theta_0))Z]}{\mathbb{E}[Z^2]}, \quad (12)$$

where we posit a PLM as the outcome model, i.e. $Y|X, Z \sim \mathcal{N}(f(X; \theta_0) + \theta_1 Z, \sigma^2)$, and θ_0, θ_1 represent the parameters in the model (Mackey et al., 2018). We denote the parameters that interact with X and Z as θ_0 and θ_1 respectively. We further denote the set of all the parameters as $\theta = (\theta_0, \theta_1)$, and the parameterized ATE estimator as $f(X; \theta)$.

Given a feasible $\bar{p}_{x|y,z}$, the ATE estimator in Eq. 12 can be fully expressed in terms of θ and $\bar{p}_{x|y,z}, z = 0, 1$:

$$\hat{\tau}(\bar{p}_{x|y,z}; \theta) = \frac{\mathbb{E}_{Y,Z}[\mathbb{E}_{p_{x|y,z}}[(Y - f(X; \theta_0))Z]]}{\mathbb{E}[Z^2]}. \quad (13)$$

Double machine learning uses the first half of the samples to fit the model $f(X; \theta)$, and uses the second half of the samples to estimate the expectation in Eq. 13. Assuming $Y|X, Z \sim \mathcal{N}(f(X; \theta_0) + \theta_1 Z, \sigma^2)$, fitting the parameters θ using MLE results in solving the least square problem $\mathbb{E}[(Y - f(X; \theta_0) - \theta_1 Z)^2] = 0$. Differentiating w.r.t. θ , we solve for the optimal θ such that

$$|\mathbb{E}[\nabla_{\theta}(Y - f(X; \theta_0) - \theta_1 Z)^2]| = 0. \quad (14)$$

This step gives us the optimal parameter θ^* in Eq. 7. Therefore, using double machine learning, the robust optimization problem for estimating ATE with noisy covariates is in the same form as Eqs. 6 and 7, with $\hat{\tau}$ and the constraint derived in Eq. 13 and Eq. 14.

C Additional Experimental Details

This section includes further details on the experimental setup, including the model training details and the hyper-parameters tuned. All code will be made available on GitHub.

C.1 Synthetic data generation details

In this section, we include the full data generation details for the synthetic data settings.

Backdoor adjustment and IPW: With the backdoor adjustment and IPW estimators, we synthetically generate two datasets with X as the confounder.

First, to demonstrate the variability of the estimated ATE intervals, we synthetically generate a dataset with binary outcomes according to a logistic model. The data generation is as follows: we randomly generate five covariates, i.e. $X_i \stackrel{iid}{\sim} N(1, I_5)$. Then, we generate the treatment Z_i from a logistic model where $P(Z_i = 1) = \text{logit}(\alpha_0 + \alpha_1^\top X_i)$. We generate the binary outcome Y_i from a logistic outcome model, where $P(Y_i = 1) = \text{logit}(\beta_0 + \beta_1 Z_i + \beta_2^\top X_i)$. To illustrate the impact of each covariates, the coefficients of the logistic model are randomly drawn from a grid $\{-1, 1\}$. As a result, we used $\alpha_0 = -1, \alpha_1 = (1, -1, 1, 1, -1)^\top, \beta_0 = -1, \beta_1 = 1, \beta_2 = (-1, -1, -1, 1, 1)^\top$.

We further consider another synthetic dataset with a more complicated nonlinear outcome model and continuous outcomes. We use the Kang and Schafer example (Kang et al., 2007), which consists of four

unobserved covariates $U_i \stackrel{iid}{\sim} N(0, I_4)$, $i = 1, \dots, n$. They are used to generate four observed covariates X_i : $X_{i1} = \exp(U_{i1}/2)$, $X_{i2} = U_{i2}/\{1 + \exp(U_{i1})\} + 10$, $X_{i3} = (U_{i1}U_{i3} + 0.6)^3$, and $X_{i4} = (U_{i2} + U_{i4} + 20)^2$. The outcome variable Y_i is generated by $Y_i = 210 + 27.4U_{i1} + 13.72U_{i2} + 13.7U_{i3} + 13.7U_{i4} + \epsilon_i$ where $\epsilon_i \stackrel{iid}{\sim} N(0, 1)$. The treatment Z_i is generated as a Bernoulli random variable with $P(Z_i = 1) = \exp(-U_{i1} - 2U_{i2} - 0.25U_{i3} - 0.1U_{i4})$.

Frontdoor adjustment: For front adjustment, we synthetically generate two datasets, with X denoting the mediators. First, we generate a dataset with binary outcomes using a logistic model with a single mediator. We begin with generating a noiseless confounder $U_i \in \mathbb{R}^2$ which is randomly drawn from a multivariate Gaussian distribution, i.e. $U_i \stackrel{iid}{\sim} N(1, I_5)$. Then, we generate the treatment Z_i from a logistic model where $P(Z_i = 1) = \text{logit}(a_0 + a_1^\top U_i)$. We then generate a binary mediator X following a logistic model as well, i.e. $P(X_i = 1) = \text{logit}(\gamma_0 + \gamma_1^\top Z_i)$. Lastly, the binary outcome Y_i is generated as: $P(Y_i = 1) = \text{logit}(\beta_0 + \beta_1 X_i + \beta_2^\top U_i)$. The values of the coefficients are drawn from a grid. We used $a_0 = -1$, $a_1 = (1, -1, 1, 1, -1)^\top$ for generating the treatment; and $\beta_0 = 1$, $\beta_1 = -1$, $\beta_2 = (-1, -1, -1, 1, 1)^\top$ for generating the outcome; $\gamma_0 = \gamma_1 = 1$ for generating the mediator X .

Next, we generate another more complicated using a similar data generation as in Jung et al. (2020). This data generation is more complicated with multiple mediators. In this model, the unobserved confounder U_i is generated as $U_i \stackrel{iid}{\sim} N(-2, 1)$. Then, we generate the treatment Z_i by drawing from a Bernoulli distribution with $P(Z_i = 1) = \text{logit}(U_i + \epsilon_z)$, where $\epsilon_z \sim N(0, 0.5)$. We further generate five covariates as the mediators, i.e. $X \in \mathbb{R}^5$. For each entry of X , it is drawn from a Bernoulli distribution with $P(X[i] = 1) = \text{logit}(c_1 + c_2 * Z_i + \epsilon_x)$, where $\epsilon_x \sim N(-1, 1)$, and the coefficients c_1, c_2 are drawn independently from a Gaussian distribution $N(-2, 1)$. Lastly, the outcome is generated as: $Y_i \sim \text{Bern}(\text{logit}(2\beta^\top X_i + U_i + \epsilon_y))$, where $\epsilon_y \sim N(-1, 1)$, and $\beta \sim N(1, 1)$.

Generating noisy covariates: Given the true covariates, we generate noisy covariates by synthetically adding a small amount of random noise to the noiseless covariates. In this way, we have both the access to the ground truth covariates and the noisy covariates. The the ground truth covariates enables us to estimate the true ATE. For each selected example, we perturb it by adding a noise that is drawn from a Gaussian distribution to each dimension. We then evaluate the performance of the different algorithms ranging from small to large amounts of noise. In this way, for backdoor adjustment and IPW with the binary outcome dataset, we select three levels of noise with mean = 0.1/0.3/0.5 and standard deviation = 0.5/0.5/1. The same noise levels are used in the dataset for frontdoor adjustment with a single mediator. For the Kang and Schafer example, we select five levels of Gaussian noise with mean = 1/2/3/4/5 and standard deviation at 1. For frontdoor adjustment with the multi-mediator dataset, we generated five levels of random Gaussian noise with mean = 0.1/0.2/0.3/0.4/0.5 and standard deviations at 0.5/0.5/1/1/1. We heuristically select the TV upper bound for each noise level as 0.1/0.2/0.3/0.4/0.5.

C.2 Optimization code details

For all the simulation studies and real case studies, we performed experiments comparing the naïve approach and the robust causal approach. All optimization code was written in Python and TensorFlow.² All gradient steps were implemented using TensorFlow’s Adam optimizer. The experiments can also be reproduced using simple gradient descent without momentum. We computed full gradients over all datasets, but minibatching

²Abadi, M. et al. TensorFlow: Large-scale machine learning on heterogeneous systems, 2015. tensorflow.org.

can also be used for very large datasets. Implementations for all approaches are included in the attached code. Training time was less than 10 minutes per model on a Laptop with a 2.3 GHz 8-Core Intel Core i9 CPU.

In the experiments, we replace all expectations in the objective and constraints with finite-sample empirical versions. For the naive approach with the backdoor and IPW adjustments, we used the DoWhy Library (Sharma et al., 2019), which is publicly available online. Specifically, for backdoor adjustment, we used `backdoor.linear_regression`; for IPW, we used `backdoor.propensity_score_weighting`, which are both implemented in the DoWhy library. For RCI-NC and the naive approach with the frontdoor adjustment, we used a linear model, i.e. $f(x; \theta) = x^\top \theta$. Additionally, for the Kang and Schafer example, we standardized the dataset such that each covariate has zero mean and unit variance.

Table 4: Hyperparameters for each approach

HPARAM	VALUES TRIED	RELEVANT APPROACHES	DESCRIPTION
η_θ	{0.0001, 0.001, 0.01, 0.1}	RCI-NC; NAIVE (FRONTDOOR)	LEARNING RATE FOR θ
η_λ	{0.5, 1.0, 2.0}	RCI-NC	LEARNING RATE FOR λ
$\eta_z, z \in \{0, 1\}$	{0.001, 0.005, 0.01, 0.1}	RCI-NC	LEARNING RATE FOR \tilde{p}_z

C.3 Hyperparameters and runtime details

The hyperparameters for each approach were chosen to achieve the best performance on the coverage probability, where “best” is defined as the set of hyperparameters that achieved the highest coverage probability while satisfying all constraints relevant to the approach. The final hyperparameter values selected for each method were neither the largest nor smallest of all values tried. A list of all hyperparameters tuned and the values tried is given in Table 4.

For both Table 1 and 3 simulations, each trial for CEVAE takes around ten minutes on an Nvidia GeForce GPU. We run for five noise levels, each level has 100 pairs of clean data and noise data. For the robust algorithm, it is much more lightweight and each trial takes around 25 minutes on a 2.3 GHz 8-Core Intel Core i9 laptop.

C.4 Further case studies dataset details

ACIC dataset. We generate our dataset directly using ACIC’s data generating process. The ACIC competition does not use the original data from UCI directly, but instead generates modified versions using pre-specified data generating processes with the known true ATE. We specifically use their “modification 1” out of four different modifications of the spam email dataset, for which code is also available on the ACIC 2019 website.

Given the true covariates, we further generate noisy covariates by synthetically adding a small amount of noise at random, using a similar procedure as for the synthetic data. Specifically, we generated five levels of Gaussian noise with mean = 0.1/0.2/0.3/0.4/0.5 and standard deviations at 0.5/0.5/1/1/1.

IHDP dataset. For the IHDP dataset, we used a procedure similar to Hill (2011); Gupta et al. (2020) to simulate the mediator and the outcome with the covariates and the treatment assignment from. The

mediator X takes the form $X \sim \mathcal{N}(cZ, \sigma_{u_m}^2)$, where Z is the treatment. The outcome Y takes the form $Y \sim \mathcal{N}(aX + W\mathbf{b}, 1)$ where W is the matrix of standardized (zero mean and unit variance) covariates and values in the vector \mathbf{b} are randomly sampled (0, 1, 2, 3, 4) with probabilities (0.5, 0.2, 0.15, 0.1, 0.05). The ground truth causal effect is $c \times a$. As a setting shown in [Gupta et al. \(2020\)](#) where frontdoor adjustment outperforms backdoor adjust, we used $a = 10, c = 1, \sigma_{u_m} = 2$.

C.5 Additional experimental results

We include the plot of the ATE intervals obtained by RCI and the true ATE, and the results of the naive ATE estimator for the frontdoor adjustment estimator in Figure 2.

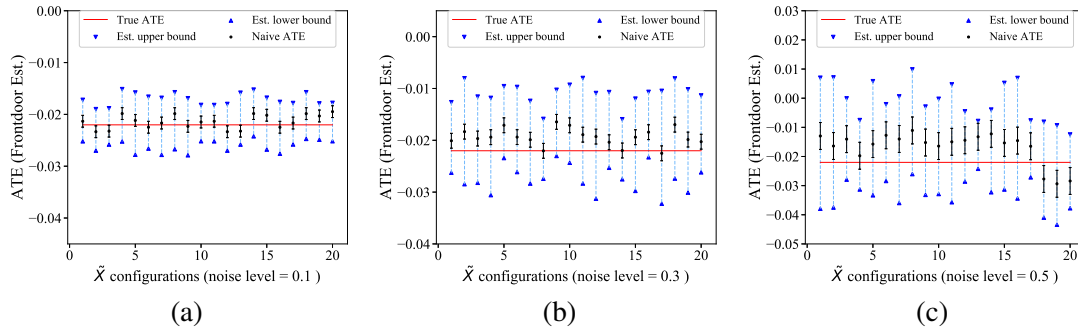


Figure 2: Partial identification of ATE with frontdoor adjustment estimators on synthetic dataset with binary outcome. The three noise levels have random Gaussian noise with mean = 0.1/0.3/0.5 and standard deviation = 0.5/0.5/1. In all plots, we compare RCI (this work) to the naive approach. The error bars indicate 95% confidence interval of the naive ATE estimation over twenty trials. *Intervals covering the true ATE is better.*